

1  
2 **Contribution of water soluble**  
3 **organic matter from multiple**  
4 **marine geographic eco-regions**  
5 **to aerosols around Antarctica**

6  
7  
8  
9 Matteo Rinaldi<sup>1</sup>, Marco Paglione<sup>1</sup>, Stefano Decesari<sup>1</sup>,  
10 Roy M. Harrison<sup>2†</sup>, David C.S. Beddows<sup>2</sup>,  
11 Jurgita Ovadnevaite<sup>3</sup>, Darius Ceburnis<sup>3</sup>, Colin D. O'Dowd<sup>3</sup>,  
12 Rafel Simó<sup>4</sup>, Manuel Dall'Osto<sup>4\*</sup>

13  
14  
15  
16  
17  
18  
19 <sup>1</sup>Institute of Atmospheric Sciences and Climate, National Research Council,  
20 Bologna, Italy.

21  
22 <sup>2</sup>National Centre for Atmospheric Science, University of Birmingham,  
23 Edgbaston, Birmingham, B15 2TT, United Kingdom

24  
25 <sup>3</sup>School of Physics and Centre for Climate and Air Pollution Studies, Ryan  
26 Institute, National University of Ireland Galway, University Road, Galway,  
27 Ireland

28  
29 <sup>4</sup>Institute of Marine Sciences, Passeig Marítim de la Barceloneta, 37-49. E-  
30 08003, Barcelona, Spain;  
31 corresponding author to Email: [dallosto@icm.csic.es](mailto:dallosto@icm.csic.es),  
32

33  
34 <sup>†</sup>Also at: Department of Environmental Sciences / Center of Excellence in  
35 Environmental Studies, King Abdulaziz University, PO Box 80203, Jeddah,  
36 21589, Saudi Arabia  
37

38  
39

40 **TOC**

41

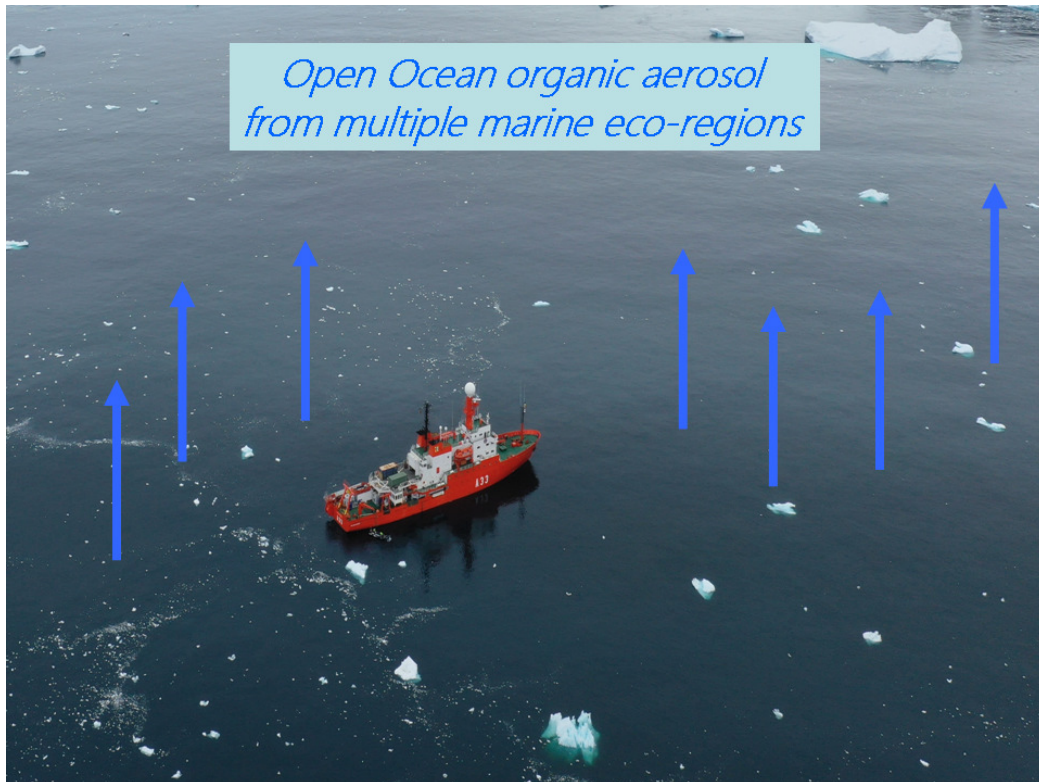
42

43

44

45

46



47

48

49

50

51

52

53

54

55

56

57

58

59 **Abstract**

60

61

62 We present shipborne measurements of size-resolved concentrations of  
63 aerosol components across ocean waters next to the Antarctic Peninsula,  
64 South Orkney Islands and South Georgia Island, evidencing aerosol features  
65 associated to distinct eco-regions. Non-methanesulfonic acid Water Soluble  
66 Organic Matter (WSOM) represented 6-8% and 11-22% of the aerosol PM<sub>1</sub>  
67 mass originated in open ocean (OO) and sea ice (SI) regions, respectively.  
68 Other major components included sea salt (86-88% OO, 24-27% SI), non sea  
69 salt sulfate (3-4% OO, 35-40% SI), and MSA (1-2% OO, 11-12% SI). The  
70 chemical composition of WSOM encompasses secondary organic  
71 components with diverse behaviors: while alkylamine concentrations were  
72 higher in SI air masses, oxalic acid showed higher concentrations in the open  
73 ocean air. Our online single-particle mass spectrometry data exclude a  
74 widespread source from sea bird colonies, while the secondary production of  
75 oxalic acid and sulfur-containing organic species via cloud processing is  
76 suggested. We claim that the potential impact of the sympagic planktonic  
77 ecosystem on aerosol composition has been overlooked in past studies, and  
78 multiple eco-regions act as distinct aerosol sources around Antarctica.

79

80

81

82

83

84

85

86

87

88

89

90

91

92

93

94

95

## 1. Introduction

96

97

98 Remote from most human influences, the Southern Ocean (SO) is one of the  
99 most pristine regions on Earth, and a window to the preindustrial atmospheric  
100 conditions and processes<sup>1-5</sup>. It is the stormiest of all oceans, and its  
101 atmospheric and oceanic circulations impact the entire Southern hemisphere  
102 and beyond. The surface of the ocean closer to the Antarctic continent  
103 undergoes an annual freezing cycle, forming a layer of sea ice that generally  
104 extends over an area ranging from  $4 \times 10^6$  km<sup>2</sup> in the summer to approximately  
105  $19 \times 10^6$  km<sup>2</sup> in late winter<sup>1</sup>. This large area increases surface albedo and  
106 controls the air-sea gas exchange. Sea ice ecosystems are also one of the  
107 largest biomes on earth, providing a stable habitat for diverse microbial  
108 assemblages<sup>2,3</sup>.

109 Currently, many unknowns remain about atmospheric and oceanographic  
110 processes in this region, and their linkages. Climate models are prone to large  
111 biases in the simulation of clouds, aerosols and air-sea exchanges<sup>4</sup>. This is  
112 largely due to the poor understanding of aerosol sources and processes in  
113 this region. Overall, two natural sources largely govern the aerosol population,  
114 sea spray (primary) and non sea salt sulfate (nssSO<sub>4</sub><sup>2-</sup>; secondary). Sea  
115 spray (mostly composed of sea salt) generated by breaking waves is often  
116 reported as the main source of supermicron aerosols in marine areas<sup>6,7</sup>.  
117 Recently, blowing snow over pack ice has been suggested to contribute sea  
118 salt aerosol in similar amounts to breaking waves<sup>8-10</sup>. The other major  
119 component of Antarctic aerosols, nssSO<sub>4</sub><sup>2-</sup>, is mainly derived from  
120 atmospheric oxidation of dimethylsulfide (DMS), a trace gas produced by  
121 marine plankton. The marine sulfur biogeochemical cycle received much  
122 attention after the proposal by Charlson et al. (1987)<sup>12</sup> that the principal  
123 source of cloud condensation nuclei (CCN) in the marine environment is  
124 DMS-derived nssSO<sub>4</sub><sup>2-</sup><sup>13</sup>. Such a hypothesis of a central role for DMS was  
125 questioned by Quinn and Bates (2011)<sup>14</sup> as the large variety of ocean-emitted

126 aerosol components was being disclosed, but mounting evidence has been  
127 collected thereafter that DMS emission chiefly contributes to aerosol formation,  
128 growth and activation as CCN over the oceans<sup>15-18</sup>. In the atmosphere, DMS  
129 is oxidized also into aerosol-prone methanesulfonic acid (MSA), which peaks  
130 in the summer and is found predominantly as methanesulfonate in the  
131 submicron size range<sup>19</sup>. Unlike  $\text{nssSO}_4^{2-}$ , which may originate also from  
132 anthropogenic and lithogenic sources, MSA has been proposed as a proxy for  
133 oceanic DMS emissions. However, the overall interpretation of MSA and  
134  $\text{nssSO}_4^{2-}$  is far less straightforward than initially thought<sup>20</sup>, given complex  
135 ecological and biogeochemical processes controlling the DMS marine  
136 emissions<sup>21</sup> and variable MSA oxidation yields<sup>22</sup>.

137 The relative roles of secondary aerosols produced from biogenic sulfur versus  
138 primary sea-spray aerosols in regulating cloudiness above the SO is still a  
139 matter of debate<sup>23-27</sup>. Mc Coy et al. (2015)<sup>25</sup> reported observational data  
140 indicating a significant spatial correlation between regions of elevated Chl-a  
141 and particle number concentrations across the SO, and showed that modeled  
142 organic mass fraction and sulfate explain  $53 \pm 22\%$  of the spatial variability in  
143 observed particle concentration, suggesting that primary marine organic  
144 aerosols are important in this region, similarly to other remote marine  
145 regions<sup>28</sup>. Despite the increasing awareness of their importance,  
146 measurements of organic components in SO aerosols are scarcer than  
147 inorganic measurements, and the overall apportionment of primary versus  
148 secondary marine aerosol in the southern hemisphere is not known. First  
149 observations of organic carbon (OC) in size-segregated aerosol samples  
150 collected at a coastal site in the Weddell Sea (Virkkula et al., 2006)<sup>29</sup> showed  
151 that MSA represented only a few % of the substantial amount of OC observed  
152 in the submicron fraction. However, Zorn et al (2008)<sup>30</sup> showed that MSA  
153 dominated Antarctic OC, whereas non-MSA organic compounds dominated  
154 SO OC. Recent measurements over the SO (43°S–70°S) and the Amundsen  
155 Sea (70°S–75°S) showed that Water Insoluble Organic Carbon (WIOC)  
156 accounted for 75% and 73% of aerosol total organic carbon in the two regions,  
157 respectively<sup>31</sup>. In the Amundsen Sea, WIOC concentrations correlated with  
158 the relative biomass of a phytoplankton species (*Phaeocystis antarctica*) that  
159 produces extracellular polysaccharide mucus. Whilst sympagic and pelagic

160 plankton biomass controls biological productivity and the organic mass budget  
161 of the Southern Hemisphere<sup>2,3</sup>, including organic emissions to the atmosphere,  
162 insular terrestrial biomass emissions contain large amounts of OC<sup>32-34</sup>.  
163 Here, we report atmospheric measurements during a 42 day cruise in the SO  
164 near Antarctica. We previously showed that the microbiota of sea ice and the  
165 sea ice-influenced ocean can be a source of atmospheric organic nitrogen  
166 (ON), specifically low molecular weight alkylamines<sup>35</sup>. In a follow-up paper, we  
167 reported a specific analysis of the primary ON aerosol detected by bubble  
168 bursting chamber experiments on board, and also showed that alkylamines  
169 form in the ambient aerosol by secondary processes involving volatilization  
170 from the ocean surface and re-condensation onto acidic aerosol particles<sup>36</sup>.  
171 Using valuable high time resolution data from the same campaign, and  
172 selecting 12 pseudo-steady state periods (where aerosol microphysical  
173 properties varied less than 20% over eight hours), Fossum et al (2018)<sup>27</sup>  
174 evaluated the relative contributions of primary and secondary aerosols to SO  
175 cloud condensation nuclei, and concluded that both sea salt and non-sea-salt  
176 sulfate were major CCN components. In the selected cases studied, non MSA  
177 organics contributed in the range 2-10% of aerosol mass.  
178 In the present work, we (1) report the aerosol water soluble fraction  
179 composition for the whole campaign; (2) report the size-resolved  
180 concentrations of oxalic acid and alkyl amines in PM<sub>10</sub> aerosols; (3) discuss  
181 the mixing state of oxalic acid by means of single particle mass spectrometry;  
182 and (4) discuss the processes and sources responsible for the measured  
183 patterns, stressing that multiple eco regions govern the aerosol population  
184 numbers and composition. Such detailed chemical characterization of the  
185 water soluble fraction of marine aerosol, including tracers of secondary  
186 aerosol formation processes, has never been achieved before close to the  
187 Weddell Sea region. We highlight that water soluble aerosol components  
188 contribute to aerosol hygroscopicity and influence the ability of particles to  
189 activate into cloud droplets, therefore being climate relevant. The role of  
190 water-soluble organics in these processes in the Antarctic atmosphere is far to  
191 being understood, mainly due to the lack of quantitative observations.  
192

## 2 Methodology

### 195 **The Cruise.**

196 We conducted extensive aerosol measurements on board of the RV  
197 Hesperides from January 2 to February 11, 2015 under the project PEGASO  
198 (Plankton-derived Emissions of trace Gases and Aerosols in the Southern  
199 Ocean). Different air masses were sampled, including the regions of Antarctic  
200 Peninsula, South Orkney, and South Georgia Islands.

### 202 **Aerosol offline measurements.**

204 Off-line aerosol samples were collected on the upper deck by using a 5-stage  
205 Berner impactor (hereafter BI5; type LPI80, Hauke; cut-offs at 0.06, 0.14, 0.42,  
206 1.2, 3.5 and 10  $\mu\text{m}$ ) and a high volume  $\text{PM}_{10}$  sampler (hereafter HIVOL;  
207 TECORA). Ion chromatography was used for the quantification of water-  
208 soluble inorganic ions, oxalic acid and low molecular weight alkyl-amines  
209 (methyl-, ethyl-, dimethyl-, diethyl- and trimethylamine)<sup>37</sup> in the BI5 water  
210 extracts, while an elemental analyzer (Shimadzu TOC-5000A) was used to  
211 quantify the water-soluble organic carbon content both of the impactor stages  
212 and of the HIVOL filters. The water soluble organic carbon content was  
213 measured on both kinds of samples to assess the impact of the sampling  
214 technique upon the measured value. Indeed, impactor samples may be  
215 subject to negative artifacts due to loss of semi-volatiles at the low operating  
216 pressure and to bouncing, while HIVOL samples on quartz filters may be  
217 affected by positive artifacts<sup>38</sup>.

218 Sampling was allowed only when the samplers were upwind the ship exhaust  
219 with a relative wind speed threshold of 5  $\text{m s}^{-1}$ . Due to the necessity of  
220 collecting sufficient amounts of samples for detailed chemical analyses,  
221 sampling time was of the order of  $\sim 50$  h for each sample. Samples were  
222 stored at  $-20$   $^{\circ}\text{C}$  until the chemical analyses. One field blank per sample was  
223 collected during the cruise and the concentrations were corrected for the  
224 blank values, which resulted negligible for amines and oxalate. A carbon-to-  
225 mass conversion factor of 2 was used to estimate the WSOM from organic

226 carbon measurements. This value is in line with state-of-the-art marine  
227 organic aerosol measurements<sup>39</sup>. The non-sea-salt fraction of aerosol  
228 chemical components was derived based on the standard seawater chemical  
229 composition using Na<sup>+</sup> as the sea-salt tracer.

230

### 231 **Aerosol online measurements.**

232

233 The online instruments<sup>34</sup> were kept inside the bow of the ship, sampling was  
234 done with an purposely designed inlet, 9m in length followed by a cyclon with  
235 a cut-off of approximately 5µm at a flow rate of 5 L min<sup>-1</sup>. All downstream  
236 online instruments were isokinetically subsampling from it and dried to below  
237 40% relative humidity. The ATOFMS (model 3800-100, TSI, Inc.) allowed  
238 collection of mass spectra (both positive and negative) of single particles  
239 roughly between 500 and 1500 nm. The ATOFMS mass spectra were  
240 imported into Yet Another ATOFMS Data Analyzer (YAADA), and adaptive  
241 resonance theory neural network, ART-2a (learning rate 0.05, vigilance factor  
242 0.85, and 20 iterations) was run<sup>40</sup>. The size resolved non-refractory chemical  
243 composition of submicron aerosol particles was measured with an Aerodyne  
244 High Resolution Time of Flight Aerosol Mass Spectrometer (HR-ToF-AMS,  
245 Aerodyne, Billerica, MA)<sup>41</sup>, hereafter indicated as AMS.

246

247

### 248 **Bioregion classification**

249

250 We collected aerosol data in the areas of the Antarctic Peninsula, South  
251 Orkney, and South Georgia Islands. We ran 117 air mass back trajectories  
252 (6h resolution, 42 days) and classified them into two broad source regions  
253 according to the characteristics of the overflown areas: “open ocean” (OO)  
254 and “sea ice” (SI). Out of the 6 samples analyzed, PE24, PE28 and PE06  
255 were assigned to OO, and PE09, PE13 and PE18 were assigned to SI<sup>35</sup>. A  
256 detailed characterization of the air mass history, ground type contribution and  
257 water soluble organic features of each sample have been presented in  
258 Decesari et al.<sup>42</sup>, where a map of the sampling locations can also be found.  
259 As we have previously showed<sup>35,36,42</sup>, SI samples are influenced by aerosol



260 precursors emitted by the peculiar microbiota thriving in sea ice and sea ice-  
261 influenced waters, while OO samples are representative of the open Ocean  
262 biota. This results in distinct chemical compositions, which we will investigate  
263 in detail below.

264

## 265 **3 Results**

266

### 267 **3.1 Overall aerosol chemical composition**

268

269 Six shipborne aerosol filters are reported in this study. Figure SI1 and SI2  
270 show the remarkable similarity among the sub-micron OO and SI samples  
271 (within the same group).

272 The average concentrations of the PM<sub>1</sub> aerosol water soluble fraction in the  
273 OO and SI samples are shown in Figure 1 and reported in Tables SI1. Sea  
274 salt dominates the PM<sub>1</sub> water soluble fraction in OO samples, with average  
275 concentrations of  $2.39 \pm 2.36 \mu\text{g m}^{-3}$  (n=3; min, max: 0.79-5.1  $\mu\text{g m}^{-3}$ )  
276 representing on average 87% of the mass. In the SI region, sea salt  
277 concentrations were ten fold lower, average of  $0.198 \pm 0.056 \mu\text{g m}^{-3}$  (n=3; min,  
278 max: 0.143-0.254  $\mu\text{g m}^{-3}$ ), representing on average only 25% of the aerosol  
279 water soluble mass. By contrast, in the SI region the dominant species was  
280  $\text{nssSO}_4^{2-}$ , with average concentrations of  $0.295 \pm 0.061 \mu\text{g m}^{-3}$  (n=3; min, max:  
281  $0.228$ - $0.348 \mu\text{g m}^{-3}$ ) representing on average 37% of the water soluble  
282 fraction. This was the third lowest species in OO air masses, with average  
283 concentrations of  $0.099 \pm 0.014 \mu\text{g m}^{-3}$  (n=3; min, max: 0.087-0.114  $\mu\text{g m}^{-3}$ )  
284 representing on average only 4% of the aerosol water soluble mass.

285 As expected, MSA exhibited similar patterns to  $\text{nssSO}_4^{2-}$ . Higher  
286 concentrations were seen from the SI region, with average concentrations of  
287  $0.088 \pm 0.032 \mu\text{g m}^{-3}$  (n=3; min, max: 0.061-0.123  $\mu\text{g m}^{-3}$ ) representing on  
288 average 11% of the water soluble fraction. High MSA concentrations over the  
289 Weddell Sea were previously attributed to emissions from the margine ice  
290 zone biota<sup>35,36,42</sup> in agreement with the global MSA climatology<sup>43</sup>. In the OO  
291 region, average concentration was  $0.043 \pm 0.012 \mu\text{g m}^{-3}$  (n=3; min, max: 0.036-  
292  $0.057 \mu\text{g m}^{-3}$ ), representing on average 2% of the aerosol water soluble mass.

293 Minor concentrations of ammonium were found for the SI region, average of  
294  $0.068 \pm 0.017 \mu\text{g m}^{-3}$  ( $n=3$ ; min, max:  $0.055$ - $0.087 \mu\text{g m}^{-3}$ ), which represented  
295 on average 9% of the water soluble fraction ( $n=3$ ; min, max: 7-10%). These  
296 were much lower in the OO region, as previously discussed in Dall'Ósto et al.  
297 (2017)<sup>35</sup>: average of  $0.027 \pm 0.005 \mu\text{g m}^{-3}$  ( $n=3$ ; min, max:  $0.022$ - $0.031 \mu\text{g m}^{-3}$ ),  
298 representing on average 2% of the water soluble mass ( $n=3$ ; min, max: 0-3%).  
299 Low ammonium concentrations made the submicron aerosol particles rather  
300 acidic as in many other remote regions.

301 A key observation was that non-MSA organic compounds (see Methods)  
302 represented an important aerosol component. The average non-MSA WSOM  
303 concentration from the BI5 was  $0.083 \pm 0.022 \mu\text{g m}^{-3}$  ( $n=3$ ; min, max:  $0.058$ -  
304  $0.10 \mu\text{g m}^{-3}$ ) and  $0.17 \pm 0.02$  ( $n=3$ ; min, max:  $0.15$ - $0.19 \mu\text{g m}^{-3}$ ) in SI and OO  
305 regions, respectively, while from the HIVOL samplers concentrations as high  
306 as  $0.19 \pm 0.05$  (SI,  $n=3$ ; min, max:  $0.21$ - $0.22 \mu\text{g m}^{-3}$ ) and  $0.21 \pm 0.05$  (OO,  $n=3$ ;  
307 min, max:  $0.17$ - $0.26 \mu\text{g m}^{-3}$ ) were obtained. Consequently, non-MSA-WSOM  
308 accounted for 11% ( $n = 3$ ; min, max: 9-16%) and 6% ( $n=3$ ; min, max: 3-13%)  
309 of total sub-micrometer water soluble mass in SI and OO regions, respectively,  
310 when considering the BI5 results, and 22% ( $n=3$ ; min, max; 18-27%) and 8%  
311 ( $n=3$ ; min, max: 4-15%), using the HIVOL data. Although the concentration  
312 differences between the two datasets are notable (particularly for the Si  
313 region), the non-MSA WSOM was the third most abundant component in SI,  
314 and the second in OO, independent of the sampling technique.

315 Parallel AMS measurements performed during the cruise<sup>27,35</sup> were averaged  
316 over the filter sampling times in order to provide a further evaluation of the  
317 organic aerosol concentration over the two regions. An excellent agreement  
318 was observed for MSA concentrations between AMS and BI5 samples ( $n = 6$ ;  
319 slope: 1.04; R: 0.66), while more significant differences were reported for the  
320 total organics. Comparing the non-MSA organic aerosol concentration by  
321 AMS with the non-MSA-WSOM measured on the BI5 samples, we got a slope  
322 of 0.53 ( $n=6$ ; R: 0.74, OM/OC = 2, see Par. 2.), indicating at least a factor two  
323 overestimation of the organic fraction on the BI5 samples with respect to AMS  
324 measurements. The overestimation was obviously higher if we compare the  
325 AMS with the HIVOL samples ( $n=6$ ; slope: 0.33, R: 0.56). Accordingly, if we  
326 assume that all the organics measured by the AMS contribute to the WSOM

327 measured offline, a reduction of the average non-MSA WSOM contribution  
328 over the SI region is obtained, from the range 11-22% by offline  
329 measurements, down to 8%.

330 This discrepancy between the sub-micrometre non-MSA organic aerosol  
331 quantification by offline and online techniques is consistent with the existing  
332 literature. Virkkula et al. (2006)<sup>29</sup> reported a high contribution of non-MSA  
333 organics in Antarctic samples (~50% of PM<sub>1</sub> mass) by offline chemical  
334 analyses, while Zorn et al. (2008)<sup>30</sup> reported a negligible non-MSA organic  
335 contribution in sub-micrometre Antarctic aerosol through online AMS  
336 measurements. Although the existing measurements are too scarce to derive  
337 any sound conclusion, the evidenced tendency is worthy of investigation and  
338 proves the necessity for further organic aerosol characterization studies over  
339 Antarctica.

340 Considering the PM<sub>10</sub> size range (Table SI2), sea salt dominated in both OO  
341 and SI samples, with average concentrations of 7.93±3.99 µg m<sup>-3</sup> (n=3; min,  
342 max: 5.20-12.51 µg m<sup>-3</sup>) and 2.17±0.83 µg m<sup>-3</sup> (n=3; min, max: 1.22-2.77 µg  
343 m<sup>-3</sup>) respectively, representing on average 94 and 78% of the aerosol water  
344 soluble mass.

345 Whilst the speciation of individual organic compounds was treated in a  
346 separate paper<sup>42</sup>, the next section discusses two chemicals of interest as  
347 markers of secondary aerosol sources.

348

## 349 **3.2 Alkylamine and oxalate measurements**

350

351 In this Section, we present the atmospheric concentrations of selected  
352 secondary aerosol formation process tracers: alkyl amines and oxalic acid.  
353 The former have been associated to secondary aerosol formation based on  
354 acid-base reactions<sup>37</sup>, including new particle formation<sup>35</sup>. The latter was  
355 identified as one of the most abundant single oxygenated compounds in many  
356 marine aerosol studies at different latitudes<sup>44-48</sup>. All the tracers were  
357 characterized by high quantification precision even at the low aerosol  
358 concentrations typical of Antarctica.

359

### 360 **3.2.1. Aerosol size-resolved mass concentrations**

361

362 Figure 2 shows that alkylamines were 5 times higher (t-test, significantly  
363 different,  $p < 0.01$ ) in aerosols from the SI region ( $n=3$ ;  $9.1 \pm 4.5 \text{ ng m}^{-3}$ ) than  
364 from the OO regions ( $n=3$ ;  $1.8 \pm 1.1 \text{ ng m}^{-3}$ ). In a previous paper<sup>35</sup> we had  
365 reported alkylamines only in  $\text{PM}_1$  aerosols, here we present the  $\text{PM}_{10}$   
366 concentrations. Contrasting with the amines, oxalate concentrations were 9  
367 times higher (t-test, significantly different,  $p < 0.05$ ) in OO ( $n=3$ ;  $1.98 \pm 1.44 \text{ ng}$   
368  $\text{m}^{-3}$ ) than in the SI ( $n=3$ ;  $0.20 \pm 0.09 \text{ ng m}^{-3}$ ) region (Figure 2a).

369 Concerning their size distributions, clear differences were seen (Figure 2b).  
370 Whilst amines occurred mainly in the fine mode, the oxalate size distribution  
371 was different between regions. In SI samples, the sub-micron oxalate  
372 concentration was below detection limit in two samples out of three, while  
373 non-negligible concentrations were always detected in the 1.2-3.5  $\mu\text{m}$  size  
374 range, resulting in the coarse-mode dominated distribution of Figure 2. In OO  
375 samples, the oxalate distribution peaked in fine particles (0.42-1.2 $\mu\text{m}$ ). Very  
376 few measurements of oxalate in the SO exist. Xu et al (2013)<sup>49</sup> reported low  
377 concentrations,  $3.8 \pm 3.8 \text{ ngm}^{-3}$  (range: 0 to 9.1), over the SO, and  $2.2 \pm 1.5$   
378  $\text{ngm}^{-3}$  (range: 0 to 4.6) over coastal Antarctica. These results were in line with  
379 data collected in Aboa Station<sup>29</sup> and in the region of  $>50^\circ\text{S}, 130^\circ\text{E}-150^\circ\text{E}$ <sup>49</sup>. In  
380 this latter study, oxalate size distributions over the SO were bimodal, with  
381 peak at  $<0.49 \mu\text{m}$  and 0.95–1.5  $\mu\text{m}$ , whereas over coastal East Antarctica  
382 oxalate concentration peaked at 0.56–1.8  $\mu\text{m}$ .

383

### 384 **3.2.2 Mixing state of oxalate containing particles**

385

386 In this section we investigate the aerosol mixing state, broadly defined as the  
387 distribution of the chemical component within the aerosol population. In  
388 Dall'Osto et al., (2019)<sup>36</sup> we compared ATOFMS spectra of particles  
389 generated by bubbling melted sea ice with those produced by bubbling  
390 surface sea water. Here, we only consider the mass spectra of ambient  
391 aerosols. We expanded the analysis by running ART-2a on mass spectra  
392 containing a peak ( $m/z$  -89,  $[(\text{C}_2\text{O}_4\text{H})\text{H}]^-$ , approximately 1,300 single particle  
393 mass spectra) representative of oxalic acid<sup>51</sup>. The small peak at  $m/z$  179 is  
394 attributed to the oxalic acid dimer  $[(\text{C}_2\text{O}_4\text{H})_2\text{H}]^-$ , which is commonly observed

395 in the spectra of oxalic acid standards. Unfortunately, the temporal trends of  
396 the ATOFMS particles detected did not allow differentiation of the SI and OO  
397 regions due to low counts and poor statistic. Nevertheless - broadly - three  
398 particle types were seen:

399 (a) ATOOFMS Na-OX (about a quarter of the total mass spectra identified): Sea  
400 spray particles containing organic carbon including oxalic acid. Peaks at  $m/z$   
401 23 ( $\text{Na}^+$ ),  $m/z$  24 ( $\text{Mg}^{++}$ ),  $m/z$  39 ( $\text{K}^+$ ) (positive mass spectra) and  $m/z$  -16 [ $\text{O}^-$ ],  
402 -17 [ $\text{OH}^-$ ], -35 ( $\text{Cl}$ ), -46 [ $\text{Na}_2^-$ ], 62 [ $\text{Na}_2\text{O}^+$ ], and 63 [ $\text{Na}_2\text{OH}^+$ ] consistent with  
403 sea salt in sea spray (Figure 3a). The negative ion mass spectrum shows  
404 prominent peaks at  $m/z$  -26 [ $\text{CN}^-$ ] and  $m/z$  -42 [ $\text{CNO}^-$ ], indicating that all  
405 particle types presented were internally mixed with organo-nitrogen species.  
406 In the negative spectra, putative peaks of oxalate ( $m/z$  -89) are seen also with  
407 larger mass peaks, likely due to unidentified large chemical compounds. This  
408 particle type likely corresponds to degraded primary marine organic aerosols  
409 internally mixed with sea spray.

410 (b) ATOOFMS biogenic-OX (about a quarter of the total mass spectra identified).  
411 Peaks due to  $\text{Na}^+$  ( $m/z$  23),  $\text{K}^+$  ( $m/z$  39) and phosphate ( $m/z$  -63 [ $\text{PO}_2^-$ ] and  
412  $m/z$  -79 [ $\text{PO}_3^-$ ]) characterize this particle type (Figure 3b). The ATOFMS has  
413 already proved to be a good tool to separate dust (mainly Ca-rich or Al-Si rich)  
414 and biological particles<sup>52,53</sup>. Briefly, biological mass spectral signatures can be  
415 differentiated from crustal dust on the basis of abundant organic and  
416 phosphorus ions, as well as a lack of key dust markers, such as aluminium  
417 and silicates. Additionally to the peak of oxalate ( $m/z$  -89) a strong peak at  $m/z$   
418 114 can be seen, previously demonstrated to be preserved in particles that  
419 contain amine salts and that have undergone photo-oxidation<sup>54,55</sup>. This  
420 particle type may correspond to biogenic material in general, but not enough  
421 mass spectra (about a dozen) were collected to obtain more information.

422 (c) ATOOFMS SOA-OX (about half of the total mass spectra identified). This  
423 particle type was seen associated with secondary organic components in both  
424 positive and negative mass spectra (Figure 3c). Beside the previously  
425 described peaks associated with amines and oxalic acid, a unique peak at  $m/z$   
426 59, ( $[\text{N}(\text{CH}_3)_3]^+$ ) is attributed to trimethylamine (TMA). Previous studies  
427 showed that cloud/fog processing can increase gas-to-particle partitioning of  
428 TMA<sup>56</sup>, and potentially form non-salt organic aerosols<sup>57</sup>. The unique mass

429 series of  $m/z$  -81, -97 and  $m/z$  -111 is due to species  $[\text{HSO}_3]^-$ ,  $[\text{HSO}_4]^-$  and  
430  $[\text{HOCH}_2\text{SO}_3]^-$ . ATOFMS particle spectra of this type have previously been  
431 shown to arise from hydroxymethanesulphonate in both laboratory studies  
432 and field experiments<sup>58,59</sup>. Minor peaks can also be seen at  $m/z$  58, 74, and  
433 128, which were previously attributed to alkyl ammonium nitrate salt particles  
434 formed by reaction of nitric acid and amines<sup>60</sup>.  
435 Our ATOFMS mixing state results confirm that a complex mixture of oxalate  
436 containing particles contributes to the chemical composition of Antarctic  
437 aerosol, including primary Na-containing aerosols and non-MSA marine  
438 secondary organic particles.

439

440

## 441 **4 Discussion**

442

443 WSOM was found present in non-negligible concentration during our study,  
444 although with significant uncertainty due to its dependence on the  
445 measurement technique. Even though alkylamines and oxalic acid altogether  
446 represented a minor fraction of the total water soluble organic mass (see  
447 Tables SI1 and SI2), these compounds can be used as proxies to discuss  
448 processes and sources of secondary organic aerosols in the study area.

449

### 450 **4.1 Multiple processes driving the observed aerosols patterns**

451

#### 452 **4.1.1 Amines**

453

454 Aliphatic amines are known important organic compounds in the marine  
455 atmosphere. An important contribution of biogenic amines to marine organic  
456 aerosol was first reported by Facchini et al. (2008)<sup>37</sup>, pointing to a secondary  
457 formation pathway for alkylammonium salts. Indeed, in our study the size  
458 distribution peaked in the accumulation mode and exhibited a good correlation  
459 with  $\text{nssSO}_4^{2-}$ ,  $\text{NH}_4^+$  and MSA, which is indicative of an acid-base reaction of  
460 gaseous amines with sulfuric or sulfonate acids. In our previous study<sup>35</sup> we  
461 demonstrated that the microbiota of sea ice and the sea ice-influenced ocean

462 is a source of atmospheric organic nitrogen, including low molecular weight  
463 alkylamines. In a follow up study<sup>36</sup>, thermodynamic equilibrium calculations  
464 suggested that the alkylamine shift from seawater to atmospheric secondary  
465 aerosol is driven by the very low pH expected in fine and ultrafine particles.  
466 Furthermore, a detailed analysis of single particle mass spectra of sea-spray  
467 (primary) aerosols artificially generated by bubbling seawater samples  
468 showed that in ambient aerosol the fingerprint of primary alkylamine-rich  
469 particles represents only a minor percentage (11-25%). Here we report an in-  
470 depth analysis of total aerosol mass as well as the size distribution of  
471 alkylamines, which show that these compounds occur in different aerosol  
472 modes from oxalic acid.

473 It should be kept in mind that ammonia and organic nitrogen in general -  
474 including alkylamines - may also be important contributors to new particle  
475 formation and growth in the SO. Indeed, using an unprecedented suite of  
476 instruments, Jokinen et al. (2018)<sup>61</sup> showed that ion-induced nucleation of  
477 sulfuric acid and ammonia, followed by sulfuric acid-driven growth, is the  
478 predominant mechanism for new particle formation and growth in eastern  
479 Antarctica a few hundred kilometers from the coast<sup>61</sup>. Dall'Osto et al (2017)<sup>35</sup>  
480 suggested that the microbiota of sea ice and sea ice-influenced ocean were a  
481 significant source of atmospheric nucleating particles (size of 1-3nm). It must  
482 be noted, though, that new particle formation and growth is a key process that  
483 governs particle number concentrations but does not play an important role in  
484 governing aerosol mass.

485

#### 486 **4.1.2 Oxalate**

487

488 Our study supports the existence of a natural source of oxalic acid to the  
489 marine atmosphere<sup>62,63</sup>. Previous studies<sup>44,62,63, 64, 65</sup> showed that oxalate was  
490 distributed along a wide aerosol size range, including the sub-micrometer and  
491 a super-micrometer mode. This suggests that oxalate of marine origin must be  
492 produced through a combination of processes. These may include:

493 (1) Cloud processing - from oxidation of gaseous glyoxal and mediated by  
494 particulate water, occurring over remote oceanic regions, which may  
495 contribute oxalate to submicrometer aerosols<sup>44,45, 46, 66, 67</sup>.

496

497 (2) Photochemical degradation of fatty acids of biological origin at the ocean's  
498 surface, giving rise to oxalic acid and other LMW dicarboxylic acids; these  
499 may be transferred with sea-spray particles to the atmosphere and  
500 subsequently degraded<sup>46, 48, 65, 68</sup>.

501

502 (3) Neutralization of gaseous oxalic acid (which may originate from points (1)  
503 or (2)) onto sea-salt particles<sup>44</sup>.

504

505 The broad size distributions of oxalate in the OO region strongly points to  
506 multiple atmospheric processes, in agreement with previous open sea  
507 observations<sup>6</sup>. By contrast, the oxalate size distribution found in the SI region -  
508 centered in the coarse mode at 1.2-3.5  $\mu\text{m}$  - could be due to the degradation  
509 of primary biogenic organic matter, emitted with sea spray<sup>62,63</sup>. According to  
510 this hypothesis, the limited importance of sea-spray emissions over the  
511 Weddell Sea<sup>35,36</sup> may explain the lower oxalate concentrations observed in SI  
512 samples with respect to OO ones. On the other hand, in Dall'Osto et al.  
513 (2019)<sup>36</sup> we have shown that sub-micron aerosol over the Weddell Sea is  
514 extremely acidic, because of the persistent fine-mode sulfate and  
515 methanesulfonic acid particles and the low liquid water content (LWC) ( $\text{pH}_{\text{SI}}$   
516 = 1.4;  $\text{pH}_{\text{OO}}$  = 6.6). The coarse size distribution of oxalate in this region may,  
517 therefore, be driven by the fine aerosol acidity, which would favour the  
518 accumulation of oxalate in the more alkaline coarse mode<sup>69</sup>. This is the  
519 simplest explanation, which probably accounts for much of the best known  
520 mechanism pattern in the oxalic acid size distribution.

521 It is also possible that alternative pathways exist, including cloud and fog  
522 processing, as discussed in point (1) above. An example of a real time event  
523 of this process was recorded in the evening of the 14th January 2014 and it is  
524 presented in Figure S14. The two aerosol size distribution modes indicative of  
525 cloud processing<sup>70</sup> can be observed during the event. This event occurred in



526 the marginal sea ice region, the research vessel was about 75Km from the  
527 closest coast of the little island of Coronation (South Orkneys). Figure SI5  
528 shows that all air masses were travelling over open ocean and not terrestrial  
529 zones before arriving at the ship. Furthermore, the case study was seen in air  
530 masses that were the most affected by sea ice and the marginal sea ice zone  
531 (Fig. SI5). A clear growth of the smaller mode from 38nm to 43nm was seen  
532 over five hours ( $1 \text{ nm h}^{-1}$ ; not shown), in concomitance with an increase of  
533 Relative Humidity due to foggy-cloudy conditions. By contrast, the decrease of  
534 the larger mode (from 105 nm to 87 nm) was likely due to the higher activation  
535 of large aerosol due to higher RH. Immediately after the onset of fog, the  
536 number of ATOFMS counts attributed to the SOA-OX particle type increased.  
537 After the event, the two size modes returned to about 38-40 nm and 181-190  
538 nm. The latter mode was likely due to cloud processing (Hoppel mode<sup>70</sup>),  
539 which transforms organic and inorganic compounds and shifts the size  
540 distribution to large accumulation mode sizes. After about 4-7am on the 15th  
541 January 2015 air masses changed, shifting towards West Pacific air masses,  
542 hence different aerosols were sampled and the event track was lost.  
543 Recently, Kim et al., (2019)<sup>71</sup> demonstrated that aqueous reactions in  
544 atmospheric droplets can significantly modify aerosol composition and  
545 contribute to the formation of oxygenated and nitrogen-containing organic  
546 compounds in atmospheric aerosol particles. Our study shows that chemical  
547 reactions involving organic compounds of biogenic origin (acid-base  
548 neutralization and oxidation reactions) - likely related to marginal sea ice  
549 zones - are also occurring in the Antarctic region, and aerosol chemical  
550 composition may be more complex than solely sulfate and sea spray.

551

## 552 **4.2 Marine vs terrestrial inputs of ammonia, amines and organic aerosol**

553

554 According to our previous studies<sup>35,36</sup>, elevated alkylamine concentrations  
555 originate from melted sea ice and sea-ice-influenced waters. These could  
556 result from degradation of quaternary amine osmolytes, which we also found  
557 in sympagic plankton. Regarding oxalate, the higher abundance in OO  
558 samples suggests that this aerosol component is less related to the coastal  
559 and marginal sea-ice zone.

560 An important open question for Antarctic aerosol is the relative role of marine  
561 versus terrestrial sources of organic matter (including organic nitrogen) and  
562 ammonia, whose answer is obscured by the scarcity of existing  
563 measurements. Recently, Liu et al (2018)<sup>34</sup> showed that atmospheric aerosol  
564 natural organic matter (OM) from a coastal location was 150 times higher in  
565 summer than in winter. Natural sources that included marine sea spray and  
566 seabird emissions contributed 56% OM in summer but only 3% in winter. The  
567 “marine source” was identified by high hydroxyl group fractions, and the  
568 “seabird source” was related to ammonium and an organic nitrogen peak  
569 associated with coastal penguin emissions<sup>34</sup>. In Bird Island, South Georgia,  
570 Schmale et al. (2013)<sup>33</sup> also showed strong influence of sea bird colonies.  
571 Legrand et al. (2012)<sup>72</sup> reported oxalate enrichment in aerosols at Dumont  
572 d’Urville Station, which was associated with the high levels of gaseous  
573 ammonia in the atmosphere. It was suggested that seabirds and mammals in  
574 coastal Antarctica could be sources of aerosol oxalate. This idea had also  
575 been discussed in Legrand et al. (1998)<sup>61</sup>, where ornithogenic soil was  
576 proposed to be a source of oxalate in aerosols. Therefore, oxalate would be  
577 produced and released together with ammonia upon bacterial decomposition  
578 of uric acid. However, it was also stressed that the relationship between  
579 gaseous nitrogen (or carbon)-derived species and emitted oxalate aerosol  
580 was likely a complex one<sup>73-74</sup>. Legrand et al. (1998)<sup>32</sup> and Jourdain and  
581 Legrand (2002)<sup>675</sup> proposed  $nssK^+$  and  $nssCa^{2+}$  as tracers for ornithogenic  
582 soil (defined as guano-enriched soil) emissions. Based on the proposed  
583 metrics, we can exclude any significant contribution from bird colony  
584 emissions in SI and, more obviously OO, samples. In fact, the  $K^+/Cl^-$  weight  
585 ratio in SI and OO samples is  $0.021 \pm 0.003$  and  $0.020 \pm 0.002$ , respectively,  
586 much closer to the seawater value (0.021) than to the proposed values for  
587 ornithogenic soils (0.23-1.4). Similarly, the  $Ca^{2+}/C^-$  weight ratio is  $0.026 \pm 0.002$   
588 and  $0.026 \pm 0.0003$ , against a seawater reference value of 0.021 and an  
589 ornithogenic soil value of 0.045. Finally, the formula for calculating the amount  
590 of potassium related to ornithogenic soil emissions ( $K_{or}$ ), proposed by  
591 Jourdain and Legrand (2002)<sup>75</sup>, yielded negative values in both SI and OO  
592 samples, demonstrating a tendency for  $K^+$  depletion and certainly not an  
593 enrichment.

594 The results presented in this study, together with our previous works from the  
595 same sampling cruise<sup>35,36,42</sup> show that alkylamines and oxalic acid have  
596 different spatially located sources in the investigated area, with the former  
597 being more related to sympagic emissions connected with sea-ice melting and  
598 sea-ice influenced waters, and the latter being more related to pelagic  
599 emissions. This suggests that aerosol chemical composition, and likely  
600 physical properties, is strictly related to the biological environment  
601 characterizing the source region<sup>35,36,42</sup>. Aerosol samples reported in this study  
602 showed no major relation with seabird emissions, even though this does not  
603 exclude that this source may be significant in other Antarctic coastal  
604 environments (eco-regions).

605

#### 606 **4.3 Considerations under a changing climate perspective**

607

608 The Antarctic region possesses a substantial spatial heterogeneity across  
609 marine, terrestrial and freshwater biomes, with productivity and biodiversity  
610 patchiness superimposed on strong environmental gradients<sup>76</sup>. Warming  
611 climate is posing one of the greatest threats to the Antarctic environment. The  
612 Antarctic Peninsula has experienced one of the most rapid temperature rises  
613 in the Southern Hemisphere<sup>77</sup>. Antarctic terrestrial productivity and  
614 biodiversity occurs almost exclusively in ice-free areas that cover less than  
615 1% of the continent, although these could increase under a strongest forcing  
616 scenario<sup>77,78</sup>. Changes in the Antarctic environment will feed back to climate  
617 by biosphere and cryosphere exchanges with the atmosphere. Antarctica  
618 harbors extreme physical gradients such as those of incident solar radiation,  
619 UV intensity, ice cover, ocean circulation and temperature, which change over  
620 time as a consequence of global warming. The impacts of these changes on  
621 marine and terrestrial life through nutrient availability, ecophysiological  
622 adaptations, duration of the productivity and breeding seasons, migrations  
623 and location of refugia will affect biogenic emissions to the atmosphere,  
624 aerosol formation and aerosol-cloud interactions. Also physicochemical  
625 transformations of organic matter, as through exposure of snow and the sea  
626 surface microlayer to solar radiation<sup>79</sup> will impact the emission of climate-  
627 active substances to the atmosphere. Future interdisciplinary studies using

628 emerging chemical and statistical analytical techniques are required to tease  
629 out processes across spatial gradients of key environmental factors.

630

### 631 **Acknowledgements**

632

633 The study was supported by the Spanish Ministry of Economy through project  
634 BIO-NUC (CGL2013–49020-R), PI-ICE (CTM2017–89117-R) and the Ramon  
635 y Cajal fellowship (RYC-2012-11922), and by the EU through the FP7-  
636 PEOPLE-2013-IOF programme (Project number 624680, MANU – Marine  
637 Aerosol NUcleations), all to MD, and PEGASO (CTM2012-37615) to RS. We  
638 wish to thank the Spanish Armada, and particularly the captains and crew of  
639 the BIO A-33 Hesperides, for their invaluable collaboration. We are also  
640 indebted to the UTM, and especially Miki Ojeda, for logistic and technical  
641 support. The Spanish Antarctic Programme and Polar Committee provided  
642 context and advice. The National Centre for Atmospheric Science NCAS  
643 Birmingham group is funded by the UK Natural Environment Research  
644 Council. The whole PEGASO team is also acknowledged.

645

646 **References**

647

648

649 (1) Cavalieri, D.J., Parkinson, C.L., Gloersen, P., Comiso, J.C. & Zwally,  
650 H.J.. Deriving long-term time series of sea ice cover from satellite passive-  
651 microwave multisensor data sets. *Journal of Geophysical Research*, **1999** 104,  
652 15 803–15 814.

653

654 (2) Arrigo KR, Lizotte MP, Mock T. Primary producers and sea ice. *Science*,  
655 **2010**, pp. 283–326

656

657 (3) Arrigo KR, van Dijken GL, Strong AL.. Environmental controls of marine  
658 productivity hot spots around Antarctica. *J Geophys Res - Oceans* **2015**, 120:  
659 5545–5565. doi: 10.1002/2015JC010888.

660

661 (4) Hamilton DS. Natural aerosols and climate: understanding the  
662 unpolluted atmosphere to better understand the impacts of pollution. *Weather*.  
663 **2015**;70(9):264–8.

664

665 (5) Carslaw, K. S., Lee, L. A., Reddington, C. L., Pringle, K. J., Rap, A.,  
666 Forster, P. M., Mann, G.W., Spracklen, D. V., Woodhouse, M. T., Regayre, L.  
667 A., and Pierce, J. R.: Large contribution of natural aerosols to uncertainty in  
668 indirect forcing, *Nature*, **2013**, 503, 67–71,  
669 <https://doi.org/10.1038/nature12674>

670

671 (6) Rinaldi, M., Decesari, S., Finessi, E., Giulianelli, L., Carbone, C., Fuzzi,  
672 S., O'Dowd, C. D., Ceburnis, D. and Facchini, M. C.: Primary and secondary  
673 organic marine aerosol and oceanic biological activity: Recent results and 5  
674 new perspectives for future studies, *Adv. in Meteorol.*, **2010**, 2010(3642), 1–  
675 10, doi:10.1155/2010/310682,.

676

677 (7) Murphy, D. M., Froyd, K. D., Bian, H., Brock, C. A., Dibb, J. E., DiGangi,  
678 J. P., Diskin, G., Dollner, M., Kupc, A., Scheuer, E. M., Schill, G. P., Weinzierl,  
679 B., Iliamson, C. J., and Yu, P.: The distribution of sea-salt aerosol in the  
680 global troposphere, *Atmos. Chem. Phys.*, 19, 4093-4104,  
681 <https://doi.org/10.5194/acp-19-4093-2019>, 2019.

682

683 (8) Legrand, M., Preunkert, S., Wolff, E., Weller, R., Jourdain, B., and  
684 Wagenbach, D.: Year-round records of bulk and size-segregated aerosol  
685 composition in central Antarctica (Concordia site) – Part 1: Fractionation of  
686 sea-salt particles, *Atmos. Chem. Phys.*, **2017**, 17, 14039-14054,  
687 <https://doi.org/10.5194/acp-17-14039-2017>

688

689 (9) Huang, J., Jaeglé, L., and Shah, V.: Using CALIOP to constrain  
690 blowing snow emissions of sea salt aerosols over Arctic and Antarctic sea ice,  
691 *Atmos. Chem. Phys.*, **2018**, 18, 16253–16269, [https://doi.org/10.5194/acp-18-](https://doi.org/10.5194/acp-18-16253-2018)  
692 16253-2018.

693

694 (10) Giordano, M. R., Kalnajs, L. E., Goetz, J. D., Avery, A. M., Katz, E.,  
695 May, N. W., Leemon, A., Mattson, C., Pratt, K. A., and DeCarlo, P. F.: The

696 importance of blowing snow to halogen-containing aerosol in coastal  
697 Antarctica: influence of source region versus wind speed, *Atmos. Chem.*  
698 *Phys.*, **2018**, 18, 16689–16711, <https://doi.org/10.5194/acp-18-16689-2018>,  
699  
700 (11) Frey, M. M., Norris, S. J., Brooks, I. M., Anderson, P. S., Nishimura, K.,  
701 Yang, X., Jones, A. E., Nerentorp Mastromonaco, M. G., Jones, D. H., and  
702 Wolff, E. W.: First direct observation of sea salt aerosol production from  
703 blowing snow above sea ice, *Atmos. Chem. Phys.*, **2020**, 20, 2549–2578,  
704 <https://doi.org/10.5194/acp-20-2549-2020>.  
705  
706 (12) Charlson, R. J., Lovelock, J. E., Andreae, M. O. & Warren, S. G.  
707 Oceanic phytoplankton, atmospheric sulphur, cloud albedo, and climate.  
708 *Nature* **1987**, 326,655–661.  
709  
710 (13) Vallina, S. M., Simó, R., Gassó, S., de Boyer-Montégut, C., del Rio, E.,  
711 Jurado, E., and Dachs, J, Analysis of a potential “solar radiation dose–  
712 dimethylsulfide–cloud condensation nuclei” link from globally mapped  
713 seasonal correlations, *Global Biogeochem. Cycles*, **2007**. 21, GB2004,  
714 doi:10.1029/2006GB002787.  
715  
716 (14) Quinn, P. K. and Bates, T. S.: The case against climate regulation via  
717 oceanic phytoplankton sulphur emissions, *Nature*, **2011**, 480(7375), 51–56,  
718 doi:10.1038/nature10580  
719  
720 (15) Lana, A., Simó, R., Vallina, S. M. and Dachs, J.: Potential for a  
721 biogenic influence on cloud microphysics over the ocean: a correlation study  
722 with satellite-derived data, *Atmos. Chem. Phys.*, **2012**, 12(17), 7977–7993,  
723 doi:10.5194/acp-12-7977-2012  
724  
725 (16) Quinn, P. K., Coffman, D. J., Johnson, J. E., Upchurch, L. M. & Bates,  
726 T. S. Small fraction of marine cloud condensation nuclei made up of sea spray  
727 aerosol. *Nature Geoscience*. **2017**, 10, 674–679  
728 <https://doi.org/10.1038/ngeo3003>.  
729  
730 (17) Giordano, M. R., Kalnajs, L. E., Avery, A., Goetz, J. D., Davis, S. M.,  
731 and DeCarlo, P. F.: A missing source of aerosols in Antarctica – beyond long-  
732 range transport, phytoplankton, and photochemistry, *Atmos. Chem. Phys.*,  
733 **2017**, 17, 1–20, <https://doi.org/10.5194/acp-17-1-2017>  
734  
735 (18) Sanchez, K. J., Chen, C.-L., Russell, L. M., Betha, R., Liu, J., Price, D.  
736 J., Massoli, P., Ziemba, L. D., Crosbie, E. C., Moore, R. H., Mueller, M.,  
737 Schiller, S. A., Wisthaler, A., Lee, A. K. Y., Quinn, P. K., Bates, T. S., Porter,  
738 J., Bell, T. G., Saltzman, E. S., Vaillancourt, R. D. and Behrenfeld, M. J.:  
739 Substantial seasonal contribution of observed biogenic sulfate particles to  
740 cloud condensation nuclei, *Sci. Rep.*, **2018** 8(1):3235 doi:10.1038/s41598-  
741 018-21590-9,.  
742  
743 (19) Rankin, A. M. and Wolff, E. W.: A year-long record of size segregated  
744 aerosol composition at Halley, Antarctica, *J. Geophys. Res.*, **2003**, 108(D24),  
745 4775, doi:4710.1029/2003JD003993.

746  
747  
748 (20) Legrand, M., Preunkert, S., Weller, R., Zipf, L., Elsässer, C., Merchel,  
749 S., Rugel, G., and Wagenbach, D.: Year-round record of bulk and size-  
750 segregated aerosol composition in central Antarctica (Concordia site) – Part 2:  
751 Biogenic sulfur (sulfate and methanesulfonate) aerosol, *Atmos. Chem. Phys.*,  
752 **2017**, 17, 14055-14073, <https://doi.org/10.5194/acp-17-14055-2017>,  
753  
754 (21) Simó, R. and Dachs, J.: Global ocean emission of dimethylsulfide  
755 predicted from biogeophysical data, *Global Biogeochem. Cy.*, **2002** 16, 1018,  
756 <https://doi.org/10.1029/2001GB001829>  
757  
758 (22) Gondwe, M., Krol, M., Klaassen, W., Gieskes, W., and de Baar, H.:  
759 Comparison of modelled versus measured MSA: NSS SO<sub>4</sub> ratios: A global  
760 analysis, *Global Biogeochem. Cy.*, 18, GB2006,  
761 <https://doi.org/10.1029/2003GB002144>, 2004  
762  
763 (23) Meskhidze, N.; Nenes, A. Phytoplankton and cloudiness in the  
764 Southern Ocean. *Science* **2006**, 314, 1419–1423.  
765  
766 (24) Korhonen, H., Carslaw, K. S., Spracklen, D. V., Mann, G., W., and  
767 Woodhouse, M. T.: Influence of oceanic dimethyl sulfide emissions on cloud  
768 condensation nuclei concentrations and seasonality over the remote Southern  
769 Hemisphere oceans: A global model study, *J. Geophys. Res.-Atmos.*, **2008**,  
770 113, D15204, doi:10.1029/2007JD009718,  
771  
772 (25) McCoy, D. T., Burrows, S. M., Wood, R., Grosvenor, D. P., Elliott, S. M.,  
773 Ma, P.-L., Rasch, P. J., and Hartmann, D. L.: Natural aerosols explain  
774 seasonal and spatial patterns of Southern Ocean cloud albedo, *Science*  
775 *Advances* **2015**, 1, e1500157.  
776  
777 (26) Gras, J. L.; Keywood, M. Cloud condensation nuclei over the Southern  
778 Ocean: wind dependence and seasonal cycles, *Atmos. Chem. Phys.* **2017**, 17,  
779 4419–4432  
780  
781 (27) Fossum, K. N., Ovadnevaite, J., Ceburnis, D., Dall’Osto, M., Marullo, S.,  
782 Bellacicco, M., Simó, R., Liu, D., Flynn, M., Zuend, A., O’Dowd, C.:  
783 Summertime primary and secondary contributions to Southern Ocean cloud  
784 condensation nuclei, *Scientific Reports.*, **2018**, 8, 13844  
785  
786 (28) O’Dowd, C. D., Facchini, M. C., Cavalli, F., Ceburnis, D., Mircea, M.,  
787 Decesari, S., Fuzzi, S., Yoon, Y.-J. and Putaud, J.-P.: Biogenically driven  
788 organic contribution to marine aerosol, *Nature* **2004**, 431(7009), 676–680,  
789 doi:10.1038/nature02959,  
790  
791 (29) Virkkula, A., Teinilä, K., Hillamo, R., Kerminen, V.-M., Saarikoski, S.,  
792 Aurela, M., Viidanoja, J., Paatero, J., Koponen, I. K., Kulmala, M.: Chemical  
793 composition of boundary layer aerosol over the Atlantic Ocean and at an  
794 Antarctic site, *Atmos. Chem. Phys.*, **2006**, 6, 3407–3421,  
795

- 796 (30) Zorn, S. R., Drewnick, F., Schott, M., Hoffmann, T., Borrmann, S.:  
797 Characterization of the South Atlantic marine boundary layer aerosol using an  
798 aerodyne aerosol mass spectrometer, *Atmos. Chem. Phys.*, **2008** 8, 4711–  
799 4728,  
800
- 801 (31) Jung, J., Hong, S.-B., Chen, M., Hur, J., Jiao, L., Lee, Y., Park, K.,  
802 Hahm, D., Choi, J.-O., Yang, E. J., Park, J., Kim, T.-W., and Lee, S.:  
803 Characteristics of biogenically-derived aerosols over the Amundsen Sea,  
804 Antarctica, *Atmos. Chem. Phys. Discuss.*, **2019**, [https://doi.org/10.5194/acp-](https://doi.org/10.5194/acp-2019-133)  
805 2019-133. Manuscript under review for journal *Atmos. Chem. Phys.*  
806 Discussion started: 20 March 2019  
807
- 808 (32) Legrand, M., F. Ducroz, D. Wagenbach, R. Mulvaney, and J. Hall,  
809 Ammonium in coastal Antarctic aerosol and snow: Role of polar ocean  
810 and penguin emissions, *J. Geophys. Res.*, **1998**, 103, 11,043–11,056,  
811 [doi:10.1029/97JD01976](https://doi.org/10.1029/97JD01976).  
812
- 813 (33) Schmale, J., Schneider, J., Nemitz, E., Tang, Y. S., Dragosits, U.,  
814 Blackall, T. D., Trathan, P. N., Phillips, G. J., Sutton, M., Braban, C. F.: Sub-  
815 Antarctic marine aerosol: dominant contributions from biogenic sources,  
816 *Atmos. Chem. Phys.*, **2013**, 13, 8669–8694.  
817
- 818 (34) Liu, J., Dedrick, J., Russell, L. M., Senum, G. I., Uin, J., Kuang, C.,  
819 Springston, S. R., Leaitch, W. R., Aiken, A. C., and Lubin, D.: High  
820 summertime aerosol organic functional group concentrations from marine and  
821 seabird sources at Ross Island, Antarctica, during AWARE, *Atmos. Chem.*  
822 *Phys.*, **2018**, 18, 8571-8587, <https://doi.org/10.5194/acp-18-8571-2018>,  
823
- 824 (35) Dall'Osto, M., Ovadnevaite, J., Paglione, M., Beddows, D.C.S.,  
825 Ceburnis, D., Cree, C., Cortés, P., Zamanillo, M., Nunes, S.O., Pérez, G.L.,  
826 Ortega-Retuerta, E., Emelianov, M., Vaqué, D., Marrasé, C., Estrada, M.,  
827 Montserrat Sala, M., Vidal, M., Fitzsimons, M.F., Beale, R., Airs, R., Rinaldi,  
828 M., Decesari, S., Facchini, M.C., Harrison, R.M., O'Dowd, C., Simó, R.,  
829 Antarctic sea ice region as a source of biogenic organic nitrogen in aerosols.  
830 *Sci. Rep.* **2017**, 7 6047. <https://doi.org/10.1038/s41598-017-06188-x>.  
831
- 832 (36) Dall'Osto, M., Airs, R. L., Beale, R., Cree, C., Fitzsimons, M. F.,  
833 Beddows, D., Harrison, R. M., Ceburnis, D., O'Dowd, C., Rinaldi, M., Paglione,  
834 M., Nenes, A., Decesari, S., Simó, R.: Simultaneous detection of alkylamines  
835 in the surface ocean and atmosphere of the Antarctic sympagic environment,  
836 *ACS Earth Space Chem.*, **2019** 3, 5, 854-862.,  
837
- 838 (37) Facchini, M. C., Decesari, S., Rinaldi, M., Carbone, C., Finessi, E.,  
839 Mircea, M., Fuzzi, S., Moretti, F., Tagliavini, E., Ceburnis, D., O'Dowd, C. D.:  
840 Important Source of Marine Secondary Organic Aerosol from Biogenic Amines,  
841 *Environmental Science and Technology*, **2008**, 42, 9116 – 9121.  
842
- 843 (38) McMurry, P. H. A review of atmospheric aerosol measurements. *Atmos.*  
844 *Environ.* **2000**, 34, 1959-1999  
845



- 846 (39) Huang, S., Wu, Z., Poulain, L., van Pinxteren, M., Merkel, M., Assmann,  
847 D., Herrmann, H., and Wiedensohler, A.: Source apportionment of the organic  
848 aerosol over the Atlantic Ocean from 53°N to 53°S: significant contributions  
849 from marine emissions and long-range transport, *Atmos. Chem. Phys.*, **2018**,  
850 18, 18043–18062, <https://doi.org/10.5194/acp-18-18043-2018>,  
851
- 852 (40) Song, X. H., Hopke, P. K., Fergenson, D. P., and Prather, K. A.:  
853 Classification of single particles analyzed by ATOFMS using an artificial  
854 neural network, ART-2A, *Anal. Chem.*, **1999** 71, 860–865,  
855
- 856 (41) DeCarlo, P. F., Kimmel, J. R., Trimborn, A., Northway, M. J., Jayne, J.  
857 T., Aiken, A. C., Gonin, M., Fuhrer, K., Horvath, T., Docherty, K. S., Worsnop,  
858 D. R., and Jimenez, J. L.: Field-Deployable, High-Resolution, Time-of-Flight  
859 Aerosol Mass Spectrometer, *Anal. Chem.*, **2006**, 78, 8281–8289.  
860
- 861
- 862 (42) Decesari, S., Paglione, M., Rinaldi, M., Dall'Osto, M., Simó, R., Zanca,  
863 N., Volpi, F., Facchini, M. C., Hoffmann, T., Götz, S., Kampf, C. J., O'Dowd,  
864 C., Ceburnis, D., Ovadnevaite, J., and Tagliavini, E.: Shipborne  
865 measurements of Antarctic submicron organic aerosols: an NMR perspective  
866 linking multiple sources and bioregions, *Atmos. Chem. Phys.*, **2020**, 20, 4193–  
867 4207, <https://doi.org/10.5194/acp-20-4193-2020>  
868
- 869 (43) Lana, A., Bell, T. G., Simó, R., Vallina, S. M., Ballabrera-Poy, J., Kettle,  
870 A. J., Dachs, J., Bopp, L., Saltzman, E. S., Stefels, J., Johnson, J. E., and Liss,  
871 P. S.: An updated climatology of surface dimethylsulfide concentrations and  
872 emission fluxes in the global ocean, *Global Biogeochem. Cycles*, **2011**, 25,  
873 GB1004, doi:10.1029/2010gb003850.  
874
- 875 (44) Rinaldi, M., Decesari, S., Carbone, C., Finessi, E., Fuzzi, S., Ceburnis,  
876 D., O'Dowd, C. D., Sciare, J., Burrows, J. P., Vrekoussis, M., Ervens, B.,  
877 Tsigaridis, K., Facchini, M. C.: Evidence of a natural marine source of oxalic  
878 acid and a possible link to glyoxal. *J. Geophys. Res. Atmos.* **2011** 116.  
879 D16204, <http://dx.doi.org/10.1029/2011JD015659>  
880
- 881 (45) Sorooshian, A., Brechtel, F. J., Ervens, B., Feingold, G., Varutbangkul,  
882 V., Bahreini, R., Murphy, S., Holloway, J. S., Atlas, E. L., Anlauf, K., Buzorius,  
883 G., Jonsson, H., Flagan, R. C., and Seinfeld, J. H.: Oxalic acid in clear and  
884 cloudy atmospheres: Analysis of data from International Consortium for  
885 Atmospheric Research on Transport and Transformation 2004, *J. Geophys.*  
886 *Res.*, **2006**, 111, D23, doi:10.1029/2005JD006880,  
887
- 888 (46) Miyazaki, Y., Kawamura, K., and Sawano, M.: Size distributions and  
889 chemical characterization of water soluble organic aerosols over the western  
890 North Pacific in summer, *J. Geophys. Res.*, **2010**, 115, D23210,  
891 doi:10.1029/2010JD014439.  
892
- 893 (47) Mochida, M., Umemoto, N., Kawamura, K., and Uematsu, M.: Bimodal  
894 size distribution of C<sub>2</sub>–C<sub>4</sub> dicarboxylic acids in the marine aerosols, *Geophys.*  
895 *Res. Lett.*, **2003**, 30(13), 1672, doi:10.1029/2003GL017451.

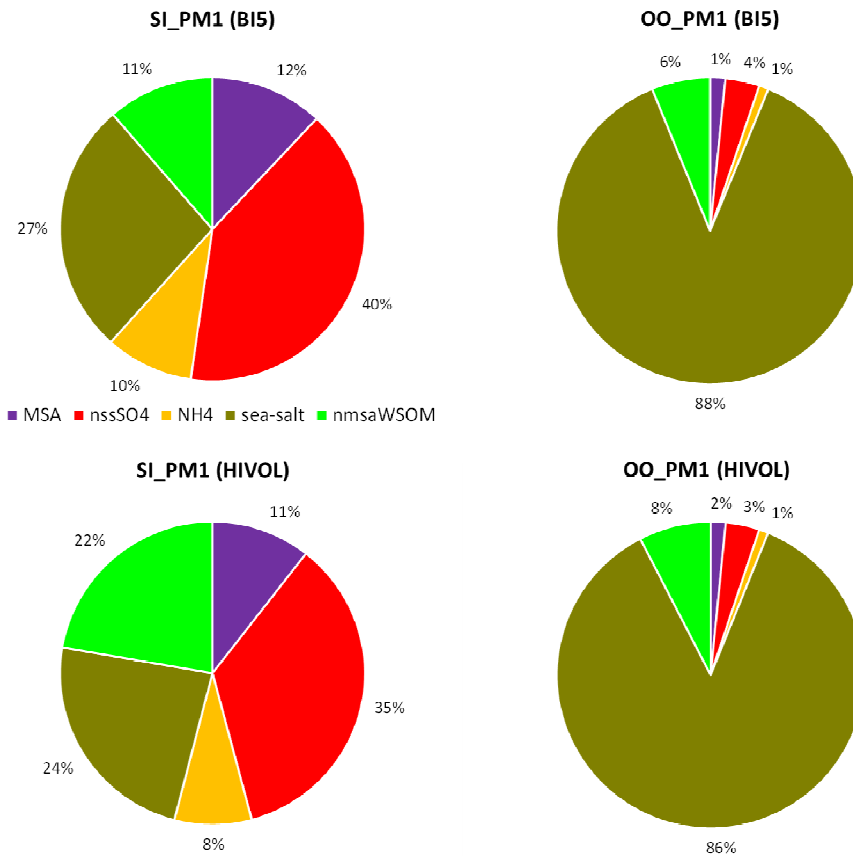
896  
897 (48) Kawamura, K., and F. Sakaguchi, Molecular distributions of water  
898 soluble dicarboxylic acids in marine aerosols over the Pacific Ocean including  
899 tropics, *J. Geophys. Res.*, **1999**, 104(D3), 3501–3509,  
900 doi:10.1029/1998JD100041  
901  
902  
903 (49) Xu, G., Y. Gao, Q. Lin, W. Li, and L. Chen, Characteristics of water-  
904 soluble inorganic and organic ions in aerosols over the Southern Ocean and  
905 coastal East Antarctica during austral summer, *J. Geophys. Res. Atmos.*,  
906 **2013** 118,13,303–13,318, doi:10.1002/2013JD019496  
907  
908 (50) Wang, H., K. Kawamura, and K. Yamazaki, Water-soluble dicarboxylic  
909 acids, ketoacids and dicarbonyls in the atmospheric aerosols over the  
910 Southern Ocean and western Pacific Ocean, *J. Atmos. Chem.*, **2006**, 53(1),  
911 43–61,doi:10.1007/s10874-006-1479-4.  
912  
913 (51) Sullivan R. C. and Prather, K. A.: Investigations of the diurnal cycle and  
914 mixing state of oxalic acid in individual particles in Asian aerosol outflow,  
915 *Environ. Sci. Technol.*, **2007**, 41, 8062–8069.  
916  
917 (52) Fergenson, D.P., Pitesky, M.E., Tobias, H.J., Steele, P.T., Czerwieniec,  
918 G.A., Russell, D.H., Lebrilla, C.B., Horn, J.M., Coffee, K.R., Srivastava, A.,  
919 Pillai, S.P., Shih, M.-T., Hall, H.L., Ramponi, A.J., Chang, J.T., Langlois, R.G.,  
920 Estacio, P.L., Hadley, R.T., Frank, M., Gard, E.E. Reagentless detection and  
921 classification of individual bioaerosol particles in seconds. *Anal. Chem.*, **2004**,  
922 76, 373–378.  
923  
924 (53) Pratt, K., DeMott, P.J., French, J.R., Wang, Z., Westphal, D.L.,  
925 Heymsfield, A.J., Twohy, C.H., Prenni, A.J., Prather, K.A.,. Situ detection of  
926 biological particles in cloud ice-crystals. *Nat. Geosci.* **2009**, 2, pages398–401  
927 <https://doi.org/10.1038/ngeo521>  
928  
929 (54) Healy, R.M., Evans, G.J., Murphy, M., Sierau, B., Arndt, J.,  
930 McGillicuddy, E., O'Connor, I.P., Sodeau, J.R., Wenger, J.C., Single-particle  
931 speciation of alkylamines in ambient aerosol at five European sites. *Anal.*  
932 *Bioanal. Chem.* **2015**, 407, 5899–5909  
933  
934 (55) Dall'Osto, M., Beddows, D. C. S., McGillicuddy, E. J., Esser-Gietl, J. K.,  
935 Harrison, R. M., and Wenger, J. C., On the simultaneous deployment of two  
936 single-particle mass spectrometers at an urban background and a roadside  
937 site during SAPUSS, *Atmos. Chem. Phys.*, **2016**, 16, 9693-9710,  
938 <https://doi.org/10.5194/acp-16-9693-2016>.  
939  
940 (56) Rehbein PJG, Jeong C-H, McGuireML, Yao X, Corbin JC, EvansGJ  
941 Cloud and fog processing enhanced gas-to-particle partitioning of  
942 trimethylamine. *Environ Sci Technol* **2011**, 45(10):4346– 4352.  
943 doi:10.1021/es1042113  
944

- 945 (57) Murphy S.M., Sorooshian A., Kroll J.H., Ng N.L., Chhabra P., Tong C.,  
946 Surratt J.D., Knipping E., Flagan R.C., Seinfeld J.H., Secondary aerosol  
947 formation from atmospheric reactions of aliphatic amines. *Atmos. Chem. Phys.*  
948 2007, 7(9):2313–2337  
949
- 950 (58) Whiteaker, J. R. and Prather, K. A.: Hydroxymethanesulfonate as a  
951 tracer for fog processing of individual aerosol particles, *Atmos. Environ.*, **2003**,  
952 37, 1033–1043  
953
- 954 (59) Dall'Osto, M., Harrison, R. M., Coe, H., and Williams, P.: Real-time  
955 secondary aerosol formation during a fog event in London, *Atmos. Chem.*  
956 *Phys.*, **2009**, 9, 2459–2469, <https://doi.org/10.5194/acp-9-2459-2009>,  
957
- 958 (60) Angelino, S.; Suess, D. T.; Prather, K. A. Formation of aerosol particles  
959 from reactions of secondary and tertiary alkylamines: Characterization by  
960 aerosol time-of-flight mass spectrometry. *Environ. Sci. Technol.* **2001**, 35,  
961 3130–3138.  
962
- 963 (61) Jokinen, T., Sipilä, M., Kontkanen, J., Vakkari, V., Tisler, P., Duplissy,  
964 E.-M., Junninen, H., Kangasluoma, J., Manninen, H. E., Petäjä, T., Kulmala,  
965 M., Worsnop, D. R., Kirkby, J., Virkkula, A., and Kerminen, V.-M.: Ion-induced  
966 sulfuric acid–ammonia nucleation drives particle formation in coastal  
967 Antarctica, *Sci. Adv.*, **2018**, 4, eaat9744,  
968 <https://doi.org/10.1126/sciadv.aat9744>,  
969
- 970 (62) Kawamura, K., R. Seméré, Y. Imai, Y. Fujii, and M. Hayashi, Water  
971 soluble dicarboxylic acids and related compounds in Antarctic aerosols,  
972 *J. Geophys. Res.*, **1996**, 101(D13), 18,721–18,728, doi:10.1029/96JD01541.  
973
- 974 (63) Kawamura, K., H. Kasukabe, and L. A. Barri, Source and reaction  
975 pathways of dicarboxylic acids, ketoacids and dicarbonyls in Arctic aerosols:  
976 One year of observations, *Atmos. Environ.*, **1996**, 30(10–11), 1709–1722,  
977 doi:10.1016/1352-2310(95)00395-9.  
978
- 979 (64) Kerminen, V. - M., K. Teinilä, R. Hillamo, and T. Mäkel, Size segregated  
980 chemistry of particulate dicarboxylic acids in the Arctic atmosphere, *Atmos.*  
981 *Environ.*, **1999**, 33, 2089–2100, doi:10.1016/S1352- 2310(98)00350-1.  
982  
983
- 984 (65) Matsumoto, K., I. Nagao, H. Tanaka, H. Miyaji, T. Iida, and Y. Ikebe,  
985 Seasonal characteristics of organic and inorganic species and their size  
986 distributions in atmospheric aerosols over the northwest Pacific Ocean, *Atmos.*  
987 *Environ.*, **1998**, 32 (11), 1931–1946, doi:10.1016/S1352-2310(97)00499-8.  
988
- 989 (66) Warneck, P. In - cloud chemistry opens pathway to the formation of  
990 oxalic acid in the marine atmosphere, *Atmos. Environ.*, **2003**, 37, 2423–2427,  
991 doi:10.1016/S1352-2310(03)00136-5.  
992

- 993 (67) Crahan, K. K., D. Hegg, D. S. Covert, and H. Jonsson, An exploration  
994 of aqueous oxalic acid production in the coastal marine atmosphere, *Atmos.*  
995 *Environ.*, **2004**, 38, 3757–3764, doi:10.1016/j.atmosenv.2004.04.009.  
996
- 997 (68) Turekian, V. C., S. A. Macko, and W. C. Keene, Concentrations,  
998 isotopic compositions, and sources of size - resolved, particulate organic  
999 carbon and oxalate in near - surface marine air at Bermuda during spring, *J.*  
1000 *Geophys. Res.*, **2003**, 108(D5), 4157, doi:10.1029/2002JD002053.  
1001
- 1002
- 1003 (69) Pye, H. O. T., Nenes, A., Alexander, B., Ault, A. P., Barth, M. C., Clegg,  
1004 S. L., Collett Jr., J. L., Fahey, K. M., Hennigan, C. J., Herrmann, H.,  
1005 Kanakidou, M., Kelly, J. T., Ku, I.-T., McNeill, V. F., Riemer, N., Schaefer, T.,  
1006 Shi, G., Tilgner, A., Walker, J. T., Wang, T., Weber, R., Xing, J., Zaveri, R. A.,  
1007 and Zuend, A.: The acidity of atmospheric particles and clouds, *Atmos. Chem.*  
1008 *Phys.*, **2020**, 20, 4809–4888, <https://doi.org/10.5194/acp-20-4809-2020>.  
1009
- 1010 (70) Hoppel, W.A., Frick, G.M., Fitzgerald, J.W.,. Marine boundary layer  
1011 measurements of new-particle formation and the effects of non-precipitating  
1012 clouds have on aerosol size distribution. *J. Geophys. Res.* **1994**, 99, 14443–  
1013 14459  
1014
- 1015 (71) Kim, H., Collier, S., Ge, X., Xu, J., Sun, Y., Jiang, W., Wang, Y.,  
1016 Herckes, P., and Zhang, Q.: Chemical processing of water soluble species  
1017 and formation of secondary organic aerosol in fogs, *Atmos. Environ.*, **2019**,  
1018 200, 158–166.  
1019
- 1020 (72) Legrand, M., V. Gros, S. Preunkert, R. Sarda-Estève, A.-M. Thierry, G.  
1021 Pépy, and B. Jourdain, A reassessment of the budget of formic and acetic  
1022 acids in the boundary layer at Dumont d'Urville (coastal Antarctica): The role  
1023 of penguin emissions on the budget of several oxygenated volatile organic  
1024 compounds, *J. Geophys. Res.*, **2012**, 117, D06308,  
1025 doi:10.1029/2011JD017102  
1026
- 1027 (73) Speir, T. W., and J. C. Cowling. Ornithogenic soils of the Cape Bird  
1028 Adelie penguin rookeries, Antarctica. 1. Chemical properties, *Polar Biol.*, **1984**  
1029 2, 199–205, doi:10.1007/BF00263625.  
1030
- 1031 (74) Speir, T. W., and R. J. Ross , Ornithogenic soils of the Cape Bird  
1032 Adelie penguin rookeries, Antarctica. 2. Ammonia evolution and enzyme  
1033 activities, *Polar Biol.*, **1984**, 2, 207–212, doi:10.1007/BF00263626.  
1034
- 1035 (75) Jourdain, B., and M. Legrand. Year-round records of bulk and size  
1036 segregated aerosol composition and HCl and HNO<sub>3</sub> levels in the Dumont  
1037 d'Urville (coastal Antarctica) atmosphere: Implications for sea-salt aerosol in  
1038 the winter and summer, *J. Geophys. Res.*, **2002**, 107(D22), 4645,  
1039 doi:10.1029/2002JD002471  
1040
- 1041 (76) Convey P, Chown SL, Clarke A, Barnes DKA, Cummings V, Ducklow H,  
1042 Frati F, Green TGA, Gordon S, Griffiths H, Howard-Williams C, Huiskes AHL,

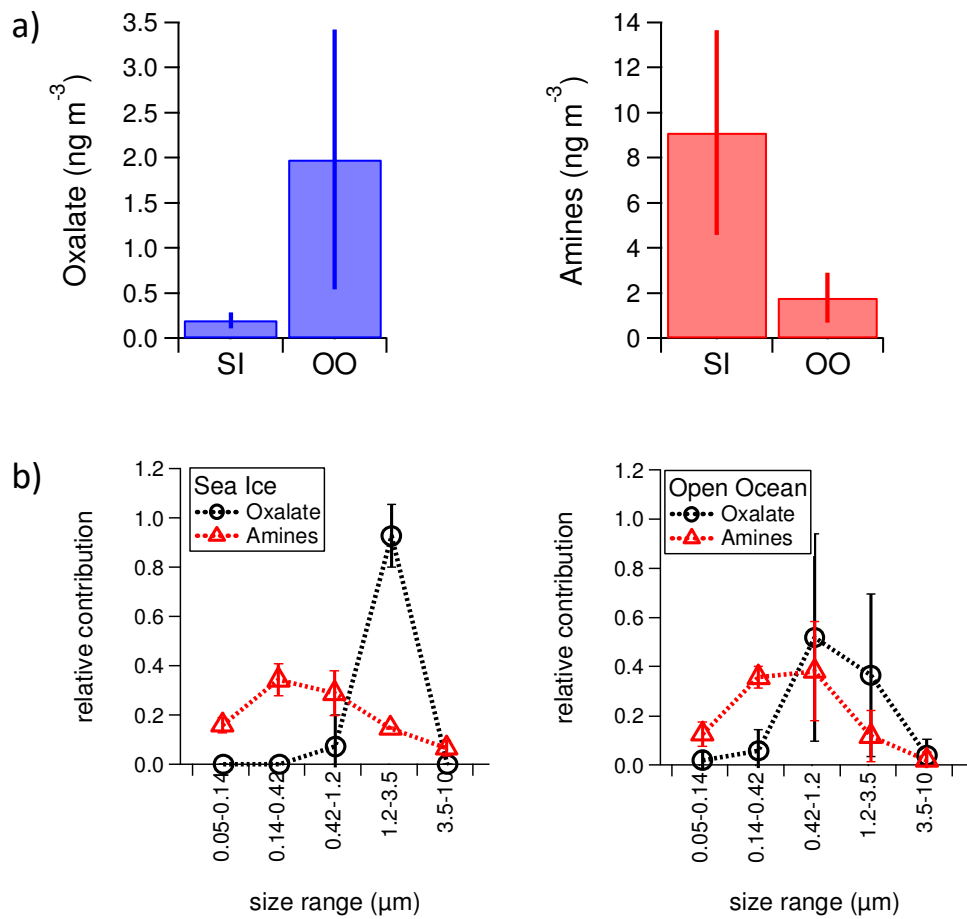
1043 Laybourn-Parry J, Lyons B, McMinn A, Peck LS, Quesada A, Schiaparelli S,  
1044 Wall D. The spatial structure of Antarctic biodiversity. *Ecol Monogr* **2014**,  
1045 84:203–244  
1046  
1047  
1048 (77) Rintoul, S. R., Chown, S. L., DeConto, R. M., England, M. H., Fricker, H.  
1049 A., Masson-Delmotte, V., Naish, T. R., Siegert, M. J., and Xavier, J. C.:  
1050 Choosing the future of Antarctica. *Nature* **2018** 558, 233–241. doi:  
1051 10.1038/s41586-018-0173-4  
1052  
1053 (78) Lee, J.R., Raymond, B., Bracegirdle, T.J., Chadès, I., Fuller, R.A.,  
1054 Shaw, J.D., Terauds, A., Climate change drives expansion of Antarctic ice-  
1055 free habitat. *Nature* **2017**, 547, 49–54.  
1056  
1057 (79) Sulzberger, B., Austin, A. T., Cory, R. M., Zepp, R. G., and Paul, N. D.:  
1058 Solar UV radiation in a changing world: roles of cryosphere-land-water-  
1059 atmosphere interfaces in global biogeochemical cycles, *Photochem. Photobio.*  
1060 **2019** S., 18, 747–774, <https://doi.org/10.1039/c8pp90063a>,.  
1061  
1062  
1063  
1064  
1065  
1066  
1067  
1068  
1069  
1070  
1071  
1072  
1073  
1074  
1075  
1076  
1077  
1078  
1079  
1080  
1081  
1082  
1083  
1084  
1085  
1086  
1087  
1088  
1089  
1090  
1091  
1092

1093  
1094  
1095  
1096  
1097  
1098  
1099



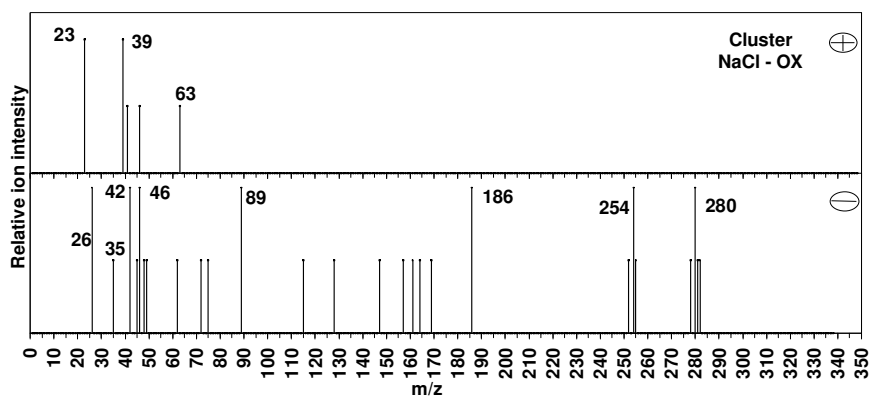
1100  
1101  
1102  
1103  
1104  
1105  
1106  
1107  
1108  
1109  
1110  
1111

**Figure 1.** Composition of PM<sub>1</sub> aerosol water soluble fraction in the sea ice influenced region (SI) versus open ocean (OO). The “BI5” pies refer to measurements performed on Berner impactor, while the “HIVOL” pies refers to the WSOM measured on the high volume samples; nmsaWSOM stands for non-MSA-WSOM.



1112  
 1113 **Figure 2.** (a) PM<sub>10</sub> concentrations of oxalate and amines in SI and OO  
 1114 samples (average and standard deviation). (b) Normalized size distributions of  
 1115 oxalate and amines for the 2 regions.

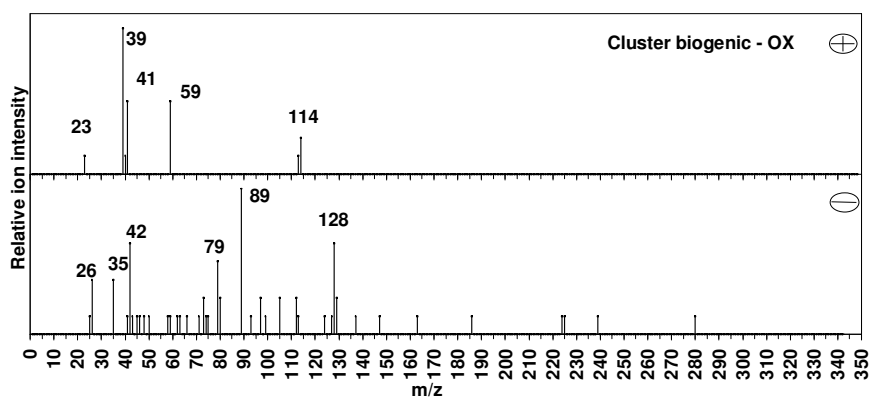
1116



1117

1118

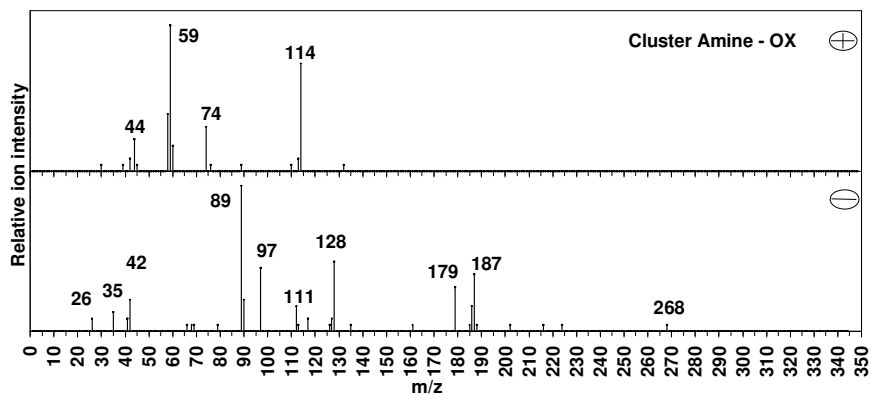
(a)



1119

1120

(b)



1121

1122

1123

(c)

1124 **Figure 3** Average Art-2a positive and negative mass spectra for (a) ATOFMS  
1125 oxalate internally mixed with sea spray, (b) ATOFMS oxalate in biogenic  
1126 particles and (c) ATOFMS oxalate in secondary organic aerosols

1127